Nonlinear Observer and Simplified Equivalent Circuit Model-based EKF-SOC Estimator of a Rechargeable $LiFePo_4$ cell

Jinhyeong Park[1], Gunwoo Kim[1], Woonki Na[2], Cheolwoo Lim[3] and Jonghoon Kim[1]
[1] Department of Electrical Engineering, Chungnam National University, Daejeon, Korea
[2] Department of Electrical and Computer Engineering, California State University, Fresno, CA, USA
[3] Satellite Research Center, Korea Advanced Institute of Science and Technology, Daejeon, Korea

***Abstract*-- The lithium iron phosphate (LFP) battery has more nonlinear characteristic than other battery type. For this reason, when we use electrical equivalent circuit model and the extended Kalman filter (EKF) for estimating the SOC, the estimation performance can be decreased in the nonlinear region. This paper proposes an advance estimation method of state of charge (SOC) for lithium iron phosphate (LFP) batteries. To improve the model accuracy, this paper utilizes the nonlinear observer for identifying the internal parameters of batteries. Furthermore, to reduce the nonlinear effect of the LFP batteries, this paper recast the Kalman process. Therefore, through the proposed method, the performance of SOC estimation can be more accurate and the computational burden is decreased when we apply the embedded system.**

***Index Terms*—Equivalent circuit model, Extended Kalman filter, LFP battery, State of charge.**

I. Introduction

Li-ion battery is a promising energy storage candidate in many fields, such as electric vehicles, portable applications, and satellites, because it has high power/energy density, long life, high voltage, and no memory effect [1]. The lithium iron phosphate (LFP) batteries have been widely used in electrical vehicle (EV) due to advantages such as light of weight, long life, safety, high energy density, high power and low self-discharge [2]. However, the LFP batteries have more nonlinear characteristics than other type of batteries because of the hysteresis characteristic [3].

In order to estimate the state of charge (SOC), many papers propose method using look-up table, Ah-counting, and model-based control method. The look-up table method establishes the function from experimental data [4]. This method has advantages which are easy implementation and low computational burden. However, this method need a lots of the experimental data for relationship function. So, it requires expensive test equipment. In case of the LFP battery, because of the nonlinear characteristics, the relationship function cannot distinguish the factor for estimating the SOC. Second, the Ah-counting method is very useful method for estimating the SOC [5]. This method uses the integration, so real-time estimation can be easily possible. This method is highly accurate, but requires a specific initial value. If the initial value is not unclear, the estimation performance is sharply decreased. From the disadvantages of the look-up table and Ah-counting method, many researches utilize the model-based control method for estimating the SOC [6] - [7]. This method has abilities that estimate the SOC in real-time, calibrate the uncertain initial value, has closed-loop control and adaptability. This method requires high performance battery model for robustness and accuracy of controller. However, the LFP battery voltage has more different characteristics according to the SOC region than general battery type as shown Fig. 1. Due this phenomenon, the performance of the electrical equivalent circuit model (EECM) is decreased. Since these nonlinear characteristics of LFP, the EECM cannot fully reflect the dynamic properties of batteries, the performance of extended Kalman filter (EKF) based on the EECM is not satisfied.

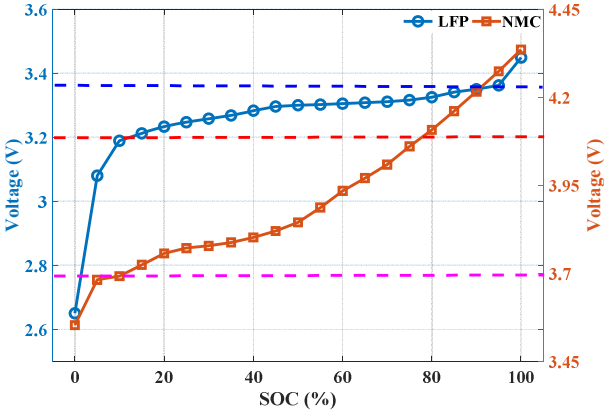

Fig. 1. Comparison of the SOC-OCV curves between the LFP and NMC batteries.

This paper proposes the strategy for enhancing the EKF performance by online parameter observer, and EECM. The online parameter observer is designed by Lyapunov stability analysis. Since the online parameter observer improves the EECM accuracy, we can eliminate unnecessary elements and simplify the EECM to reduce the computational complexity of the algorithm. Finally, the proposed method is verified by various profile.

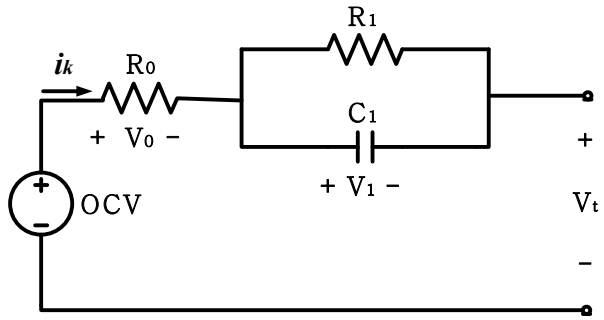

Fig. 2. Conventional equivalent electrical circuit model of Li-ion battery.

II. CONVENTIONAL BATTERY MODEL AND ALGORITHM

A. Electrical equivalent circuit model of Li-ion battery

The nonlinear characteristics of LFP batteries stand out at SOC - OCV relationship. The SOC – OCV curve of NCA batteries has linear region except for low SOC region as shown Fig. 1. However, the LFP batteries has flat period at middle SOC region (5 ~ 95%). The reason of this phenomenon is that the internal resistance of the battery has lower than high/low SOC region as shown Fig. 1. From the nonlinear result of the SOC - OCV relationship, the conventional method that calculates SOC by the SOC – OCV function has poor performance [8]. In order to estimate the SOC, the Ah-counting method is utilized as:

$$\mathrm{SOC}_{k+1} = \mathrm{SOC}_0 + (\Delta t / \mathrm{C_n}) i_k \tag{1}$$

where SOC_0 indicates the initial SOC, Δt is the time sampling of the algorithm, and i_k is the battery current.

The Ah-counting has simple mechanism and high accuracy without SOC – OCV relationship. However, this method has fatal disadvantage that is open loop system and accumulation form. From the disadvantage of Ah counting, the performance of SOC estimation is decreased when initial value is uncertain and current signal has noise signal.

The SOC, open circuit voltage (*OCV*), ohm resistance (R_0), diffusion resistance (R_1), and diffusion capacitance (C_1) is the parameter of the EECM, as shown in Fig. 2. The SOC indicates the ratio of the remaining capacity to the nominal capacity (C_n) of the battery [9].

The current to the RC parallel circuit is defined as:

$$i_{R_{diff},k+1} = \exp(-\Delta t/\tau)\cdot i_{R_{diff},k} + (1-\exp(-\Delta t/\tau))\cdot i_k \tag{2}$$

where τ is time constant.

The state of batteries is represented as:

$$x_k = [SOC_k \quad V_{diff}]^T \sim N(\hat{x}_k, P_k) \tag{3}$$

where P_k is the error covariance about the x_k. The error covariance is the indicator that shows how different from the true value.

The nonlinear state equation of battery is constructed as [10]:

$$f(x_k,u_k) = \begin{bmatrix} 1 & 0 \\ 0 & \exp(-\Delta t/\tau_k) \end{bmatrix} \times \begin{bmatrix} SOC_k \\ V_{diff,k} \end{bmatrix} + \begin{bmatrix} -\Delta t/C_n \\ R_1(1-\exp(-\Delta t/\tau_k)) \end{bmatrix} \times I_k + w^x, w^x \sim N(0,Q^x) \tag{4}$$

TABLE I
EXTENDED KALMAN FILTER ALGORITHM

Nonlinear System

$$x_k = f(x_{k-1},u_{k-1},\theta_{k-1}) + w^x_{k-1}$$
$$y^x_k = z(x_{k-1},u_{k-1},\theta_{k-1}) + w^x_{k-1} \tag{8}$$

$$w^x \sim N(0,Q^x), v^x \sim N(0,R^x) \tag{9}$$

where w^x, *and* v^x are independent, zero mean, Gaussian noise of covariance matrices R^x, and Q^x respectively.

Definition

$$A_k = \left.\frac{\partial f(x_k,u_k,\hat{\theta}^-_k)}{\partial x}\right|_{x_k=\hat{x}^+_k}$$
$$H_k = \left.\frac{\partial z(x_k,u_k,\hat{\theta}^-_k)}{\partial x}\right|_{x_k=\hat{x}^-_k} \tag{10}$$

Initialization

$$\hat{x}_0 = E(x_0), P_0 = E[(x-\hat{x}_0)(x-\hat{x}_0)^T] \tag{11}$$

For k = 1,2,… compute

Step 1: State estimation time update

$$\hat{x}^-_{k+1} = f(\hat{x}^+_k, u_k, \hat{\theta}^-_{k+1})$$
$$P^-_{k+1} = A_k P_k A_k^T + Q^x \tag{12}$$

Step 2: Measurement update for the state

$$\begin{cases} K^x_k = P^-_{k+1} H_k^T (H_k P^-_{k+1} H_k^T + R^x)^- \\ \hat{x}^+_{k+1} = \hat{x}^-_{k+1} + K^x_k (z_k - \hat{z}_k), P^+_{k+1} = (I - K_k H_k) P^-_{k+1} \end{cases} \tag{13}$$

$$z(x_k,u_k) = OCV_k(SOC_k) + I_k R_0 + V_1 + v^x$$
$$, v^x \sim N(0,R^x) \tag{5}$$

where (3) is indicate process function and (4) measurement function. Q^x is state noise of battery, and R^x is the noise of voltage sensor.

The EKF need Jacobian matrix for reflecting system variable to the algorithm. In case of the battery, the system variable is very nonlinear and arbitrary. Therefore, for linearizing the system variable, the Jacobian matrix is defined as:

$$A_k = \left.\frac{\partial f}{\partial x}\right|_{x_k=\hat{x}^+_k} = \begin{bmatrix} 1 & 0 \\ 0 & \exp(-\Delta t/\tau_k) \end{bmatrix} \tag{6}$$

$$H_k = \left.\frac{\partial z}{\partial x}\right|_{x_k=\hat{x}^-_k} = \begin{bmatrix} \left.\frac{\partial OCV}{\partial SOC}\right|_{SOC_k=S\hat{O}C^-_k} & 1 \end{bmatrix} \tag{7}$$

The EKF flow chart is shown in TABLE □. The EKF is the recursively calculate the Kalman gain and error covariance in every step time, and the Kalman gain adjust the state. First, we set to the nonlinear system function as (8) and noise parameter as (9). The system variables for calculating the Kalman gain and reflecting the system characteristic is defined as (10). Eq. (11) is that the initial state and error covariance is establish. In time update, the state and error covariance is updated as (13). In (13), the Kalman gain is calculated and state is calibrated from the Kalman gain and model error. Since the state is updated, the new error covariance is updated.

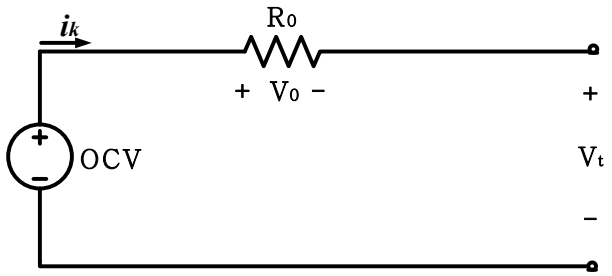

Fig. 3. Simplified equivalent electrical circuit model.

III. Proposed Method

A. Online OCV identification observer

Since the LFP batteries has nonlinear characteristics, the error of EECM can be increased using the conventional method such as linear interpolation. In order to improve the accuracy of EECM, in this paper, OCV is identified by the adaptive parameter observer reported in [11].

The OCV observer is defined as:

$$\begin{bmatrix} \dot{\hat{\partial}}_1 \\ \dot{\hat{\partial}}_2 \end{bmatrix} = \begin{bmatrix} -\alpha_1 V_0 (V_0 - \hat{V}_0) \\ \alpha_2 (V_0 - \hat{V}_0) \end{bmatrix} \tag{14}$$

where α is the gain based on the system characteristics. α_1 is set to 0.01 and α_2 to 3.6 representing the nominal voltage of the battery.

The OCV value can be estimated as:

$$\hat{OCV} = \hat{\partial}_2 / \dot{\hat{\partial}}_1 \tag{15}$$

From the nonlinear observer, the EECM accuracy and the EKF robustness can be increased in all SOC region.

B. Simplified equivalent circuit method

In the conventional EKF simultaneously calibrates SOC and V_1. In this case, the selection of Q_x can be difficult for adjusting the two variables (SOC and V_{diff}). Furthermore, the Jacobian matrix of process function need a time constant value according to the SOC. Since the LFP batteries have nonlinear characteristics, the EKF has additional method for reflecting the time constant. However, in this paper, the EKF algorithm is simplified by eliminate the time constant information as:

$$\begin{aligned} &f(SOC_k, u_k, \theta_k) = SOC_k + (-\Delta t / C_n) \times I_k \\ &+ w^x, w^x \sim N(0, Q^x) \end{aligned} \tag{16}$$

$$z(x_k, u_k) = OCV_k(SOC_k) + I_k R_0 + v^x, v^x \sim N(0, R^x) \tag{17}$$

This paper calibrates only SOC value as (12), because the OCV observer can improve the EECM accuracy. If only partial SOC information is given, it is calculated as (11), and the equation for obtaining the error covariance can be calculated as (13). The partial differentials of only SOC information are calculated as (13), and the equation for obtaining the error covariance can be modified as (14). From this equation, the Kalman filter calculations can reduce the amount of computation by reducing the portion of the matrix that contains the matrix. In addition, since it is not affected by the time constant, it becomes more robust when

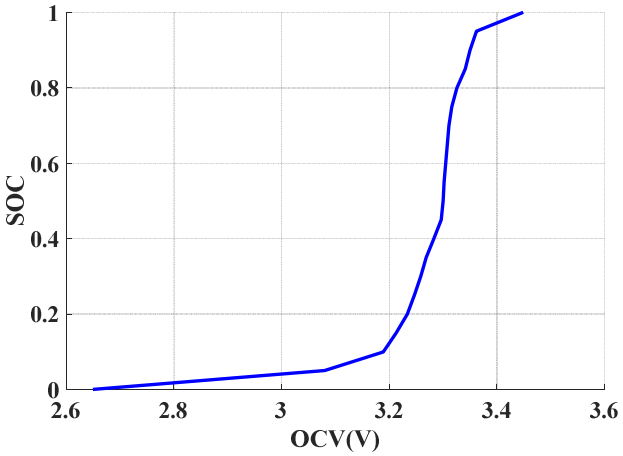

Fig. 5. OCV-SOC relationship table of the LFP cell.

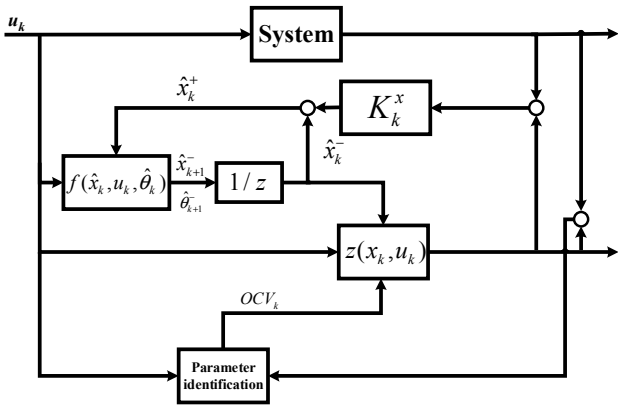

Fig. 4. Block diagram of the proposed method

estimates the SOC. Finally, to verify the proposed algorithm, the voltage and current profile are used as shown in Fig. 5.

$$S\hat{O}C_{k+1}^+ = S\hat{O}C_{k+1}^- + K_k^x (z_k - \hat{z}_k) \tag{18}$$

$$A_k = \left. \frac{\partial f}{\partial x} \right|_{x_k = \hat{x}_k^+} = 1 \tag{19}$$

$$P_{k+1}^- = P_k + Q^x \tag{20}$$

C. Initial error covariance calculation

Initial covariance affects to initial Kalman gain in (12) and (13). If initial covariance is incorrect, the overall estimation performance is decreased. In conventional method, the initial error covariance set to constant. However, since the initial SOC of the battery is uncertain, the initial error covariance has various value according to the initial SOC. To overcome this problem, this paper calculates the initial error covariance by OCV-SOC relationship as shown Fig. 5 from the experimental data. From the measure voltage (Vt), the initial SOC is calculated from Fig. 5. Through the (21), the initial covariance is estimated.

$$P_0 = (SOC_0(V_t) - S\hat{O}C_0)^2 \tag{21}$$

where $SOC_0(V_t)$ is the OCV and SOC relationship extracted from the experimental data and $S\hat{O}C_0$ is the initial SOC of the setting value in EKF.

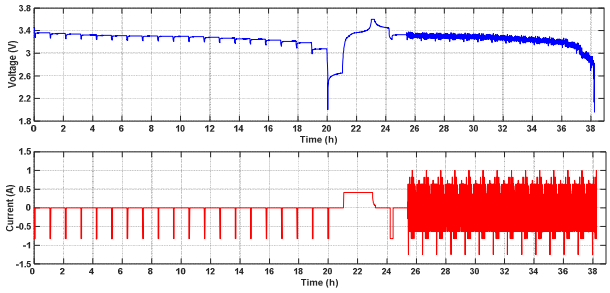

Fig. 6. Profiles of cell current and voltage under OCV and EV profile.

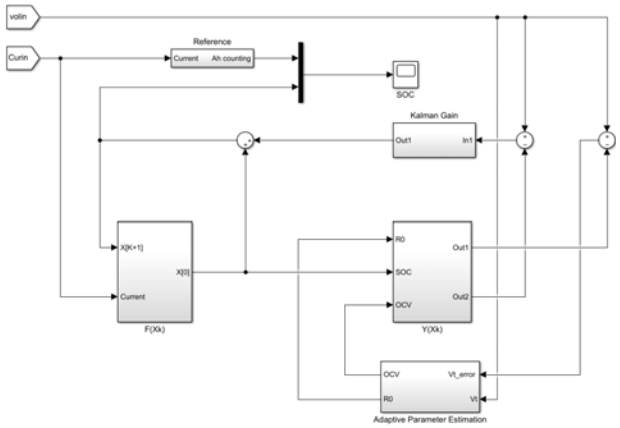

Fig. 7. EKF Matlab/Simulink model for simulation.

IV. Simulation Result

In this section, proposed method is verified by using experimental data as shown Fig. 6. The simulation is performed using Matlab/Simulink as shown Fig. 7. In order to verify the estimation performance of the proposed method according to the SOC region, it was verified through the OCV test profile. The EV profile are utilized under the various current profile to verify the robustness and estimated performance of the EKF. In addition, the influence of the error covariance and the estimated voltage error which have a great effect on the estimation performance of the EKF is analyzed.

A. Error covariance

Eq. (20) calculates the initial error covariance from the experimental data (OCV-SOC function). In order to compare the error covariance value, the Fig. 8 are shown. The estimation value is that is calculated by the Kalman filter. Eq. (20) cannot fully reflect the LFP battery's characteristics, but the tendency of the error covariance is similar between the estimation and (20) value. Therefore, since the initial error covariance is valid, the initial Kalman gain can adjust the uncertain initial SOC to true value at any initial SOC value.

B. Voltage estimation

Fig. 9 shows the graph comparing Measured and estimated voltage. The overall voltage error rate did not exceed 2%, but the error rate is different according to the test profile as shown Fig. 10. In the OCV profile, since the OCV region is long because the only discharge and rest step are repeated, it is confirmed that the voltage error is smaller than EV profile. In the EV profile, the error rate is

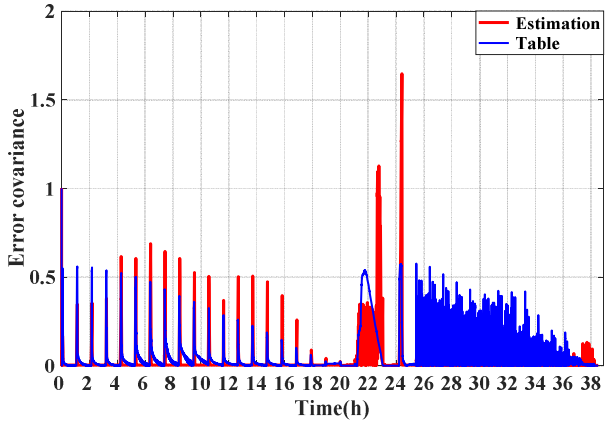

Fig. 8. Comparison of the error covariance estimation result from Kalman filter and OCV-SOC table.

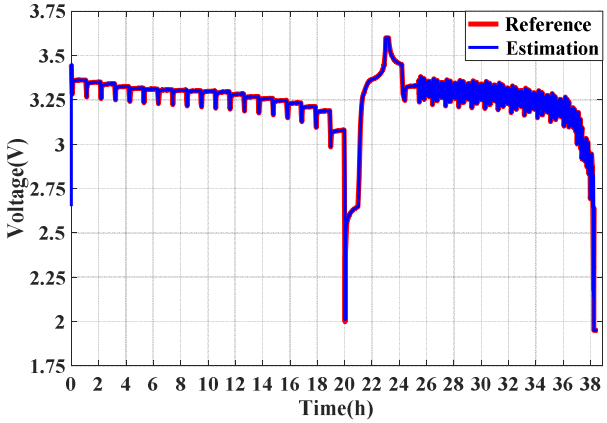

Fig. 9. Comparing the measured and estimated voltage for verifying EECM performance.

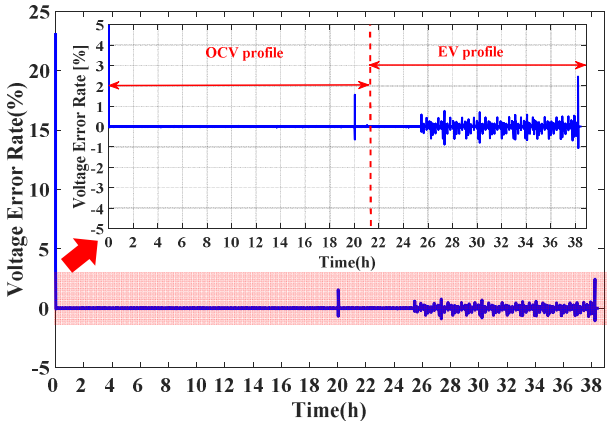

Fig. 10. Analysis the estimated voltage error rate according to the profile region.

increased due to frequent charging/discharge profile. Because the OCV region is short, the OCV observer cannot estimate the terminal voltage as much OCV profile. However, the terminal voltage is estimated within 1%. Therefore, the EECM based on the online OCV observer can be guaranteed in various profile.

C. SOC estimation

The SOC estimation result of the proposed method are shown in Fig. 11. Fig. 11. (a) shows overall estimation result and partial result for analyzing the SOC. For verifying the initial value correction, the initial value of the SOC is set to 0. In the Fig. 11. (b) is shown that the estimated SOC

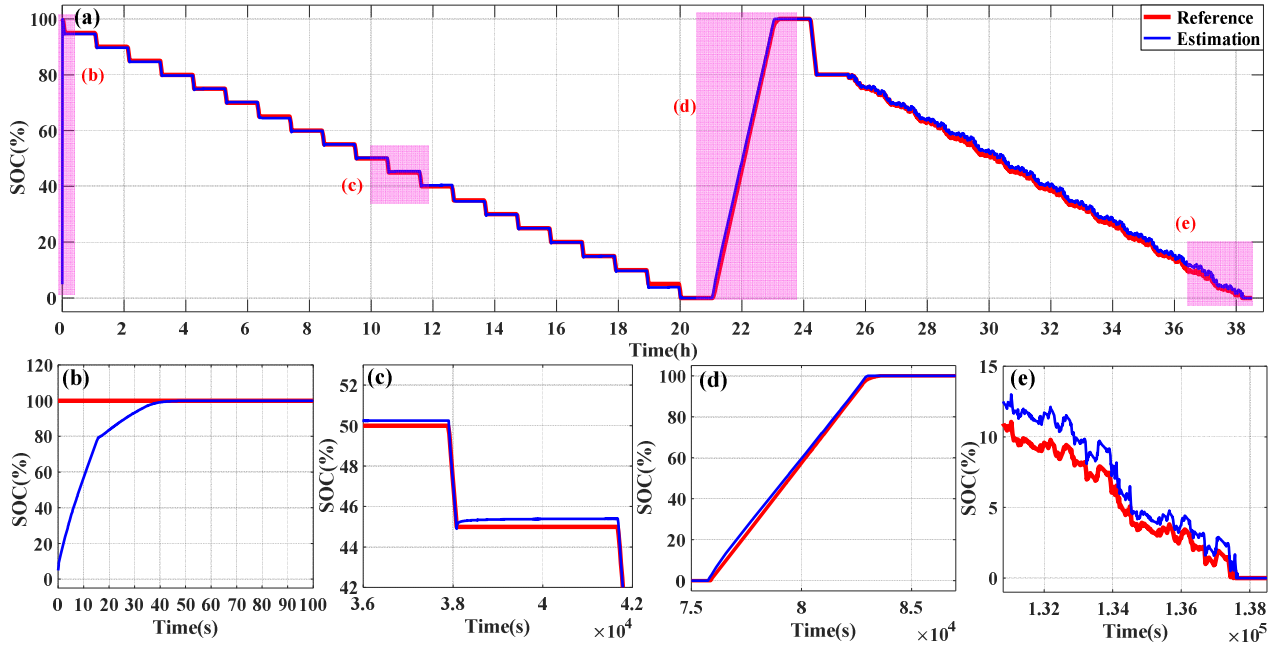

Fig. 11. SOC estimation performance comparison of proposed method and the Ah-counting. (a) the overall profile SOC estimation result, (b) initial SOC estimation region, (c) middle SOC region of the OCV profile, (d) full charging region, (e) EV profile at low SOC region.

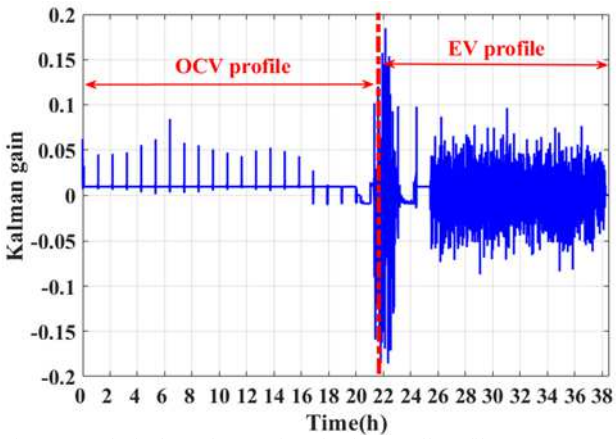

Fig. 12. Analysis the Kalman gain value in overall profile.

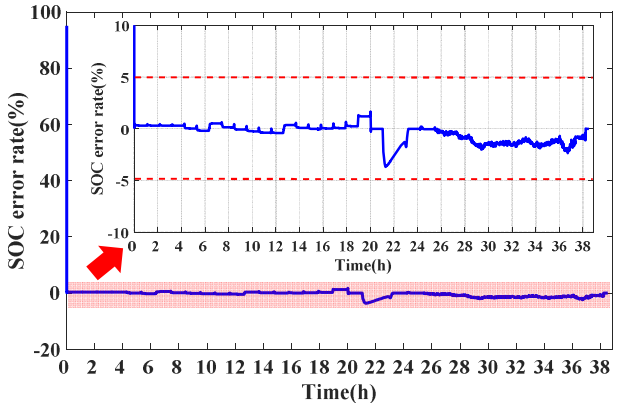

Fig. 13. Analysis the SOC error rate in overall profile.

is converged to true value within 40s. In the middle SOC region (SOC 90~10%), the voltage drop is very small. However, since EKF calibrate the SOC value using Ah-counting and voltage error, the SOC estimation result is uniform result according to the SOC region as shown Fig. 11. (c). Fig. 11. (d) represents the charging period. The error is increased comparing the other region, but it is not exceeded about 5%. This reason is that LFP battery has hysteresis characteristics when we apply charging and discharging current. In EV profile, the SOC is estimated within 3%. The SOC value is converged to true value while perform the EKF as shown Fig. 11. (d).

The voltage error is increased at EV profile as shown Fig. 10. The value of the Kalman gain is increased according to the EECM error, and the SOC value is appropriately corrected as shown Fig. 12. In the OCV profile, since the EECM error is low and current profile is static, the Kalman gain is not much change. In contrary to OCV profile, the Kalman gain is very dynamic according to the charging/discharging. From the Kalman gain, the SOC is estimated within 5%.

V. Conclusions

This approach improves the SOC estimation performance of the EKF by increasing the model accuracy and simplifying the state matrix. To improve the EECM accuracy, the nonlinear observer is used for estimating the OCV. The nonlinear component is neglected in Kalman process by recasting the state function. Through this approach, the matrix form can be decreased and algorithm can be simple than conventional method. Therefore, since the matrix component can be reduced, the computational burden in embedded system can be efficiently operated.

....

ACKNOWLEDGMENT

This work was supported by the National Research Foundation of Korea(NRF) grant funded by the Korea government (MSIT) (No. NRF-2018R1C1B6004482) and the National Research Foundation of Korea (NRF) grant funded by the Space Core Technology Development Project (No. NRF-2017M1A3A3A03016056)

REFERENCES

[1] Hannan, M. M. Hoque, A. Mohamed, and A. Ayob, ‘‘Review of energy storage systems for electric vehicle applications: Issues and challenges,’’ Renew. Sustain. Energy Rev., vol. 69, pp. 771–789, Mar. 2017.

[2] Xiaobin Zhang, Huei Peng, Hewu Wangm, and Minggao Ouyang, “Hybrid Lithium Iron Phosphate Battery and Lithium Titanate Battery Systems for Electric Buses,” IEEE TRANSACTONS ON VECULAR TECHNOLOGY, VOL. 67, 2018, pp. 956 – 965.

[3] Gregory L. Plett, “Battery Management Systems,” ARTECH HOUSE, USA, vol. 1, 2015.

[4] Einhorn M, Conte F, Kral C, Fleig J. A method for online capacity estimation of lithium ion battery cells using the state of charge and the transferred charge. IEEE Trans Ind Appl 2012.4.8, pp. 734–41.

[5] KongSoon N, Chin-Sien M, Yi-Ping C, Yao-Ching H. Enhanced coulomb counting method for estimating state-of-charge and state-of-health of lithium-ion batteries. Appl Energy 2009.8.6, pp. 1506–11.

[6] Plett G. Extended Kalman filtering for battery management systems of LiPBbased HEV battery packs-Part 3. State and parameter estimation. J Power Sources, pp. 277–92.

[7] Tian Y, Xia B, Sun W, Xu Z, Zheng W. A modified model based state of charge estimation of power lithium-ion batteries using unscented Kalman filter. J Power Sources, pp. 619–26.

[8] M.A. Hannan, M.S.H. Lipu, A.Hussain, A. Mohamed, “A review of lithium-ion battery state of charge estimation and management system in electric vehicle applications: Challenges and recommendations”, Renewable and Sustainable Energy Reviews, vol. 78, 2017, pp. 834-854.

[9] Yuejiu Zheng, Wenkai Gao, Minggao Ouyang, Languang Lu, Long Zhou and Xuebing Han, “State-of-charge inconsistency estimation of lithium-ion battery pack using mean-difference model and extended Kalman filter”, Journal of Power Sources, 383, 2018, pp. 50-58.

[10] H.S. Ramadan, M. Eecherif and F. Claude, “Extended Kalman filter for accurate state of charge estimation of lithium-based batteries: a comparative analysis”, INTERNATIONAL JOURNAL OF HYDROGEN ENEREGY, 42, 2017, pp. 29033-29046.

[11] B. Ning, B. Cao, B. Wang, Z. Zou, “Adaptive sliding mode observers for lithium-ion battery state estimation based on parameters identified online”, Energy, 153, 2018, pp. 732-742.